Thermoresponsive Nanohydrogels Cross-Linked by Gold Nanoparticles

Xueming Lian, Jie Jin, Jia Tian, and Hanying Zhao*

Key Laboratory of Functional Polymer Materials, Ministry of Education, Department of Chemistry, Nankai University, Tianjin 300071, People's Republic of China

ABSTRACT Thermoresponsive nanohydrogels cross-linked by gold nanoparticles (AuNPs) were prepared by 1,3-dipolar cycloaddition reactions and in situ reversible addition−fragmentation chain-transfer (RAFT) polymerization. In order to synthesize thermoresponsive nanohydrogels, AuNPs decorated with azide groups (AuNPs-N_3) were prepared through ligand exchange. Click reactions between AuNPs-N_3 and dialkynetrithiocarbonate yielded cross-linked AuNP aggregates. The size and cross-linking density of AuNP aggregates increased with the molar ratio of acetylene groups to azide groups. After click reactions, the absorption maximum of the plasmon band of AuNPs red-shifted to a long wavelength. Thermoresponsive nanohydrogels were prepared by in situ RAFT polymerization of *N*-isopropylacrylamide (NIPAM) using trithiocarbonate in the cross-linked AuNP aggregates as chain-transfer agents. The thermoresponsive nanohydrogels presented a low critical solution temperature at around 32 °C due to the "coil-to-globule" transition of connecting PNIPAM chains in the nanohydrogels. The size of the thermoresponsive nanohydrogels was determined by the molar ratio of acetylene groups to azide groups.

KEYWORDS: nanohydrogel • gold nanoparticles • RAFT polymerization • click reaction

INTRODUCTION

The synthesis of hydrogels has attracted extensive interest because of their great potential applications in tissue engineering, biomedical implants, drug delivery, and bionanotechnology (1−5). When the sizes of hydrogels are in the submicrometer range, they are known as nanohydrogels (6−8). Nanohydrogels can be used in polymer-based drug-delivery systems (9, 10). Various synthetic methods for the preparation of nanogels including photolithographic and micromolding methods, continuous microfluidics, modification of biopolymers, and heterogeneous free-radical and controlled/living radical polymerizations have been developed in the past decade (11). Recently, the development of hydrogels hybridized with nanosized inorganic materials has been of increasing interest in the field of materials science (12−18). Nanoparticles have found wide applications in biomedical, electronic, and optical materials as well as in catalysis. Studies on the properties of hydrogels combined with nanoparticles were reported previously (19−22). In order to develop new hybrid nanohydrogels with specific properties, new synthetic methods need to be explored. Hydrogels are generally prepared from hydrophilic polymer matrixes that are cross-linked by a physical or chemical method. The physical cross-linking includes hydrogen bonds, crystallized domains, hydrophobic interactions, stereocomplexation, temperature-induced sol−gel transition, host−guest interaction, aggregation, and self-assembly (11). Chemical cross-linking in the preparation of nanohydrogels involves chemical reactions in the presence of various difunctional or multifunctional cross-linkers (11). In the chemical cross-linking process, the cross-linkers are covalently bonded to hydrophilic polymer matrixes.

Gold nanoparticles (AuNPs) are the most stable metal nanoparticles and present many fascinating properties, such as size-related electronic and optical properties (23, 24). AuNPs can be used as elementary building blocks in the bottom-up approach of nanotechnology (25, 26). Materials with one-, two-, and three-dimensional structures can be fabricated based on AuNPs. In many cases, the collective properties of the assembled structures are expected to surpass those of the isolated nanoparticles, so the study of the self-assembly of AuNPs has aroused much interest (27, 28). To date, several different strategies have been developed to assemble AuNPs into ordered structures with unique properties. For example, self-assemblies of AuNPs based on antigene−antibody interactions (29), biotin−avidin interactions (30), the Langmuir−Blodgett technique, and molecular recognition (31), were realized, and a variety of structures were built up. One of the most useful approaches to assembling AuNPs is to cross-link the nanoparticles. Cross-linking structures of AuNPs were previously reported by some research groups. For example, Mirkin, Letsinger, and their co-workers prepared AuNP assemblies based on DNA-linked AuNPs, and they found very interesting optical properties of the materials (32, 33). Andres and co-workers studied close-packed planar arrays of AuNP aggregates, which are covalently linked to each other by rigid organic interconnects (aryldithiols or aryldiisonitriles) (34). Dithiols have been frequently used as linkers to obtain cross-linked AuNP aggregates (35, 36). Besides the use of dithiol compounds, a variety of specific interactions, chemical reactions, and polymerizations taking place on the surfaces of AuNPs can be used to prepare AuNP aggregates. For example,

* To whom correspondence should be addressed. Tel: 086-22-23498703. E-mail: hyzhao@nankai.edu.cn.
Received for review April 8, 2010 and accepted July 19, 2010

DOI: 10.1021/am1003156

Kaifer and co-workers reported the formation of large network aggregates of water-soluble AuNPs capped with thiolated γ-cyclodextrin hosts in the presence of C_{60} fullerene molecules (37). The driving force for the aggregation is the formation of inclusion complexes between two cyclodextrins on AuNPs and one molecule of C_{60}.

In the preparation of cross-linked AuNP aggregates, click chemistry is an ideal choice for its mild reaction conditions conducted in multiple solvents, tolerance to numerous functional groups, high yields, and high selectivity (38, 39). Click chemistry was used as a general route in the functionalization of AuNPs (40). For example, Jiang and co-workers used this method to detect traces of Cu^{2+} ions in solution according to a change of the solution color (41). Gole and Murphy grafted enzyme and trypsin onto the AuNPs by click chemistry (42). Peng and co-workers used click chemistry to graft PNIPAM chains onto the AuNPs (43).

In this research, AuNPs functionalized with azide groups (AuNPs-N_3) were obtained by ligand exchange. Click reactions between AuNPs-N_3 and dialkynetrithiocarbonate yielded AuNP aggregates. The reversible addition−fragmentation chain-transfer (RAFT) agent molecules connecting the neighboring AuNPs were used in the RAFT polymerization of *N*-isopropylacrylamide (NIPAM), and thermoresponsive nanohydrogels were prepared (Scheme 1). The distance between the neighboring AuNPs in the nanohydrogels can be controlled by the temperature, and smart materials with different optical properties can be obtained. AuNPs in the nanohydrogel matrix dramatically alter the properties of the composites relative to the individual components. Until now, a number of methods have been developed to incorporate AuNPs into PNIPAM hydrogels (44−46). To our knowledge, this research represents the first report on the preparation of PNIPAM/AuNP nanohydrogels with high AuNP content and a controllable interparticle distance.

EXPERIMENTAL SECTION

Materials. L-Ascorbic acid sodium salt (NaAs), 4-(dimethylamino)pyridine (DMAP; 99%), and diisopropyl azodicarboxylate (DIAD; 94%) were purchased from Alfa Aesar. *N*-[3-(Dimethylamino)propyl]-*N*′-ethylcarbodiimide hydrochloride (EDC · HCl) was purchased from Shanghai Medpep Co., Ltd. Trisodium citrate, $CuSO_4 \cdot 5H_2O$, $HAuCl_4 \cdot 4H_2O$, triphenylphosphine, and mercaptoacetic acid were purchased from Tian Jin Chemical Co. Sodium azide and 11-bromo-1-undecanol were purchased from Aldrich. All of the above chemicals were used as received. NIPAM (Aldrich) was purified by recrystallization in a toluene/hexane mixture (1:10 by weight). 4,4′-Azobis(4-cyanopentanoic acid) (ABCPA; Aldrich, 97%) was recrystallized in methanol and dried under a vacuum at room temperature. *S*,*S*′-bis(α,α′-dimethyl-α″-acetic acid)trithiocarbonate was synthesized according to the literature (47). All of the solvents were of analytical grade and were distilled before use.

Synthesis of AuNPs. AuNPs were synthesized according to the literature (48). AuNPs with an average diameter of 14 nm were prepared by the citrate-mediated reduction of $HAuCl_4$. The process was described as follows. A stirred aqueous solution of $HAuCl_4 \cdot 4H_2O$ (10 mg, 10 mL) was heated to reflux, and then a trisodium citrate solution (50 mg, 90 mL) was added quickly, which resulted in a change of color from pale yellow to deep red. After the color change, the solution was heated under reflux for 30 min and allowed to cool to room temperature.

Scheme 1. (a) Schematic Illustration of the Preparation of Thermoresponsive Nanohydrogels Based on Click Reaction and RAFT Polymerization and (b) Schematic Representation of the Bridging of Neighboring AuNPs by PNIPAM Chains Prepared by in Situ RAFT Polymerization[a]

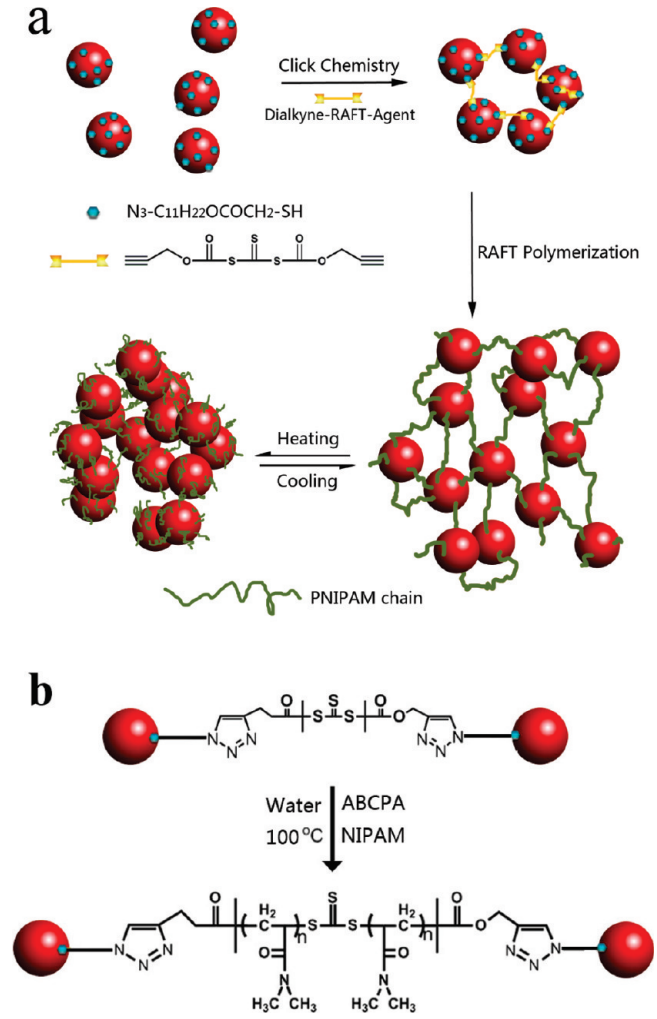

[a] In the polymerization, 4,4′-azobis(4-cyanopentanoic acid) (ABCPA) was used as free-radical initiator.

Synthesis of 11-Azido-1-Undecanol. As shown in Scheme 2a, 11-azido-1-undecanol was synthesized according to the previous literature (49). Sodium azide (1.5 g, 23.8 mmol) and 11-bromo-1-undecanol (3.0 g, 11.9 mmol) were dissolved in a mixture of acetone (50 mL) and water (10 mL), and the resulting solution was refluxed for 36 h. After acetone was removed under reduced pressure and 50 mL of water was added, the mixture was extracted three times (3 × 30 mL) with diethyl ether. The organic layer was dried over $MgSO_4$. After removal of the solvent under reduced pressure, 11-azido-1-undecanol was isolated as a colorless oil (1.9 g, 74.3% yield). ^{1}H NMR ($CDCl_3$, δ, ppm, TMS): 1.25 (14H, broad peak, $C_7\mathbf{H}_{14}$), 1.55 (4H, m, $C\mathbf{H}_2-CH_2-OH$, $C\mathbf{H}_2-CH_2-N_3$), 1.93 (1H, s, O**H**), 3.22 (2H, t, $C\mathbf{H}_2-N_3$), 3.58 (2H, t, $C\mathbf{H}_2-OH$).

Synthesis of 11-Azidoundecyl 2-Mercaptoacetate. The synthesis of 11-azidoundecyl 2-mercaptoacetate is shown in Scheme 2b. A solution of 11-azido-1-undecanol (0.3 g, 1.41 mmol) and mercaptoacetic acid (0.25 g, 2.72 mmol) in dichloromethane (6 mL) was cooled to 0 °C, and EDC · HCl (0.34 g, 2.68 mmol) and DMAP (64.8 mg, 0.53 mmol) were subsequently added. The solution was stirred at 0 °C for 2 h and at room temperature

Scheme 2. Schemes for the Synthesis of 11-Azido-1-undecanol and 11-Azidoundecyl 2-Mercaptoacetate

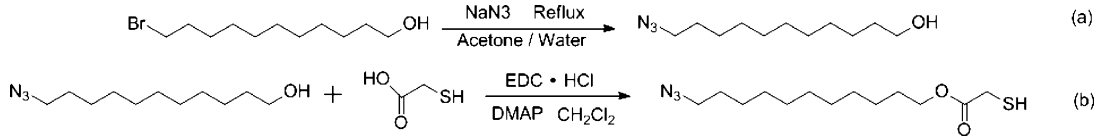

Scheme 3. Scheme for the Synthesis of Dialkynetrithiocarbonate

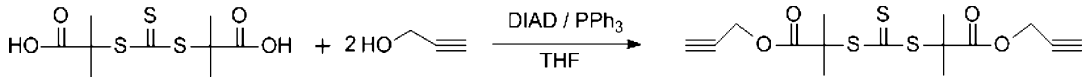

for 48 h. The reaction mixture was washed with a dilute NaOH aqueous solution (5%, 2 × 10 mL) and water (2 × 10 mL), respectively. The organic layer was dried over $MgSO_4$.. The volatiles were removed under reduced pressure, and the crude product was purified by column chromatography [eluent: 5:1 (v/v) hexanes/ethyl acetate] to afford 0.1 g (24.7% yield) of a colorless liquid. ^{1}H NMR ($CDCl_3$, δ, ppm, TMS): 1.25 (14H, broad peak, $C_7\mathbf{H}_{14}$), 1.61 (4H, m, $-C\mathbf{H}_2-CH_2-O$, $-C\mathbf{H}_2-CH_2-N_3$), 3.26 (2H, t, $-C\mathbf{H}_2-N_3$), 3.58 (2H, s, $-C\mathbf{H}_2-SH$), 4.14 (2H, t, $-CH_2-C\mathbf{H}_2-O$).

Synthesis of Dialkynetrithiocarbonate. Dialkynetrithiocarbonate was synthesized according to the previous literature (50). The synthesis of dialkynetrithiocarbonate was shown in Scheme 3. The detailed synthetic process was described as follows. A round-bottomed flask equipped with a dropping funnel was charged with *S*,*S*′-bis(α,α′-dimethyl- α″-acetic acid)trithiocarbonate (0.50 g, 1.78 mmol), propargyl alcohol (0.36 mL, 6.07 mmol), triphenylphosphine (1.48 g, 5.56 mmol), and 8 mL of anhydrous tetrahydrofuran (THF) under a nitrogen atmosphere. The flask was immersed in an ice bath, and DIAD (1.8 mL, 5.99 mmol) in 5 mL of dry THF was added dropwise. The temperature of the mixture was maintained below 10 °C. Upon completion of the addition, the solution was stirred at room temperature for 24 h and subsequently at 40 °C for 24 h. The reaction mixture was cooled to room temperature, diluted with 20 mL of dichloromethane, and washed twice with 10 mL of a saturated sodium bicarbonate aqueous solution. The combined organic layer was dried over magnesium sulfate and concentrated under vacuum. The product was purified by column chromatography [eluent: 20:1 (v/v) hexanes/ethyl acetate] to afford 0.41 g of a yellow liquid (65% yield). ^{1}H NMR ($CDCl_3$, δ, ppm, TMS): 1.68 (12H, s, $-C\mathbf{H}_3$), 2.46 (2H, s, C**H**), 4.68 (4H, s, $-C\mathbf{H}_2-$).

Synthesis of Cross-Linked AuNP Aggregates. Ligand-exchange reactions were performed by mixing 10 mL of as-prepared AuNP colloids (2.9×10^{-12} mol/mL) with 3.0 μL of a *N*,*N*-dimethylformamide (DMF) solution of 11-azidoundecyl 2-mercaptoacetate (0.04 mg/mL). The solution was stirred at room temperature for 12 h, and AuNPs-N_3 was prepared.

Click chemistry was used in the preparation of cross-linked AuNP aggregates. A typical reaction was described as follows. A DMF solution of dialkynetrithiocarbonate (2.0 μL, 1.2 mg/mL) was added to a solution with suspended AuNPs-N_3 (the molar ratio of N_3 to alkyne is about 1:30). After the solution was vigorously stirred, 3 mg of $CuSO_4 \cdot 5H_2O$ in 0.1 mL of water and 5 mg of NaAs in 0.1 mL of water were added at room temperature, sequentially. The solution became colorless, and dark precipitates could be observed in the solution. The solution was dialyzed against water for 3 days [molecular weight cutoff (MWCO) 7000 Da] to remove excess $CuSO_4 \cdot 5H_2O$ and NaAs.

Synthesis of Thermoresponsive Nanohydrogels. Thermoresponsive nanohydrogels were synthesized by the RAFT polymerization. A typical polymerization was described as follows: NIPAM (7.5 mg) and ABCPA (0.05 mg) were added into an aqueous suspension of AuNP aggregates. The solution was deoxygenated by bubbling in nitrogen gas for 1 h at room temperature. The flask was placed in an oil bath preheated to 100 °C, and the polymerization was conducted for 12 h. The polymerization was terminated by exposing the solution to air. The solution was dialyzed against water for 3 days (MWCO 14 000 Da) to remove excess monomer and initiator.

Characterization. ^{1}H NMR spectra were recorded on a Varian UNITY-plus 400 M nuclear magnetic resonance spectrometer using deuterated chloroform (Cambridge Isotope, 99.8% D + 0.03% TMS, CIL) as the solvent at room temperature. Transmission electron microscopy (TEM) images were obtained on a Tecnai G2 20S-TWIN electron microscope equipped with a model 794 CCD camera (512 × 512) at an operating voltage of 200 kV. The TEM specimens were prepared by depositing aqueous solutions on Formvar grids. The ζ potentials and hydrodynamic diameters of the thermoresponsive nanohydrogels were determined on a Brookheaven ZetaPALS (Brookhaven Instruments) at 25 and 45 °C. The scattering angle was 90°. The UV−vis spectra of AuNPs and nanohydrogels were collected on a Varian Cary 100 UV−vis spectrophotometer using a quartz cell of 1 cm path length. The samples were scanned in the range of 900−200 nm with a scanning speed of 200 nm/min.

RESULTS AND DISCUSSION

AuNPs protected by trisodium citrate were prepared according to the previous literature (48). A TEM image of AuNPs is shown in Figure 1a. A size distribution histogram is plotted in the inset of Figure 1a. Statistical analysis of the nanoparticles shows that the diameters of AuNPs range from 11 to 17 nm with a mean diameter at 14 nm. The size distribution of these nanoparticles is relatively low. Azide-functionalized AuNPs were prepared by ligand exchange of 11-azidoundecyl 2-mercaptoacetate. In order to keep AuNPs-N_3 well-dispersed in an aqueous solution, only a small amount of 11-azidoundecyl 2-mercaptoacetate was used in the ligand exchange. In this research, the molar ratio of 11-azidoundecyl 2-mercaptoacetate to AuNPs was controlled at 15:1. Because of the low content of surface azido groups on AuNPs, it is difficult to determine the number of azido groups on an AuNP by surface elemental analysis. In order to determine the number of azido groups, the alkyne pyrene was reacted with AuNPs-N_3 and the number of pyrene groups on an AuNP was determined by fluorescence analysis. Because click chemistry is a highly efficient chemical reaction, the number of pyrene groups on an AuNP is very close to that of azido groups. Our fluorescence result shows that there are 19 pyrene groups on an AuNP after the click reaction. The experimental details can be found in the Supporting Information. The average size of the AuNPs is kept unchanged after ligand exchange (Figure 1b), which means that the AuNPs do not aggregate together after ligand

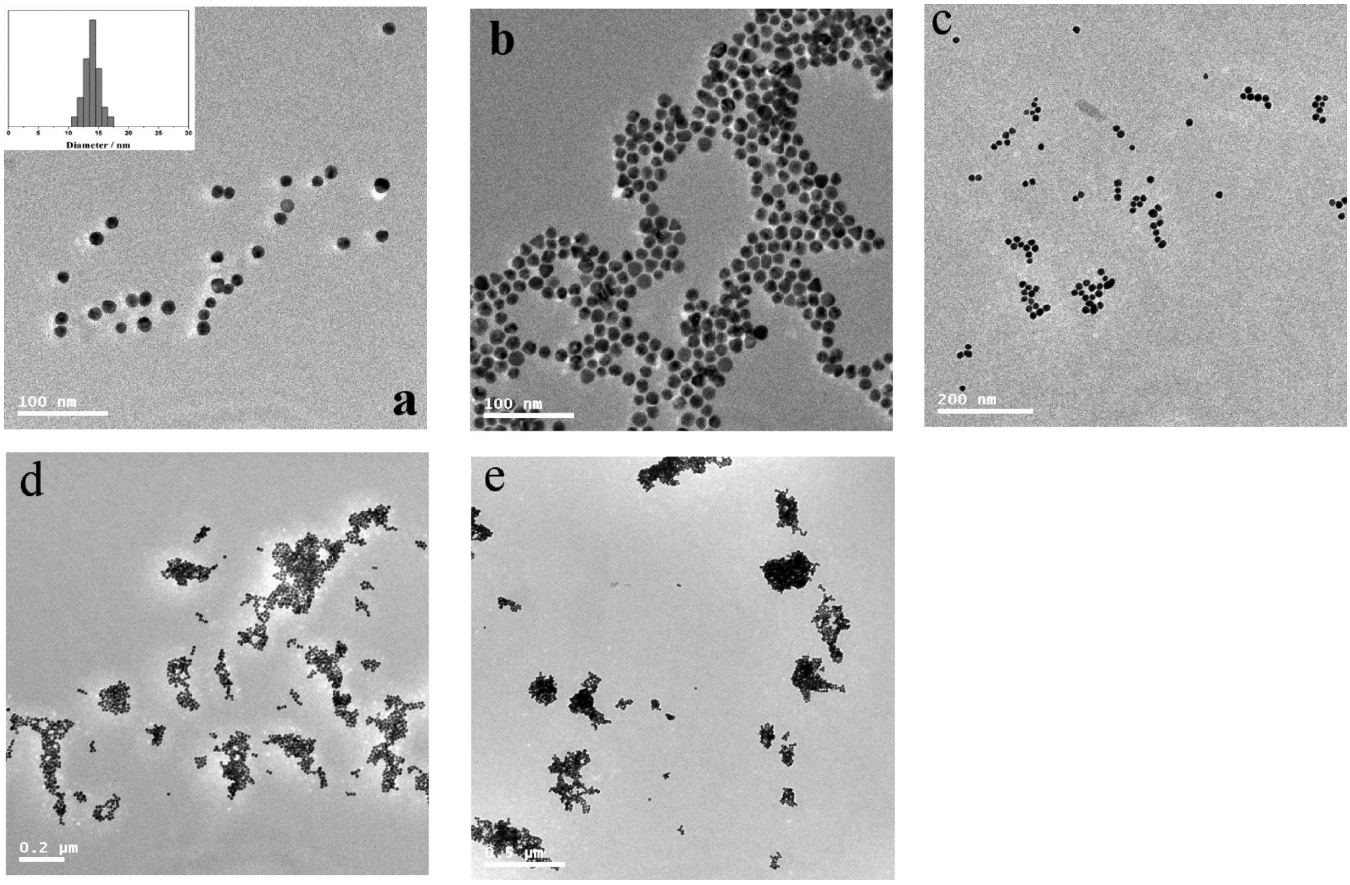

FIGURE 1. TEM images of (a) AuNPs, (b) AuNPs-N_3, and cross-linked AuNP aggregates, wherein the molar ratios of acetylene groups to azide groups are 1.5:1 (c), 15:1 (d), and 30:1 (e).

exchange. Previous researches have proven theoretically and experimentally that aggregation of the AuNPs leads to another plasmon absorption at longer wavelength when the individual nanoparticles are electronically coupled to each other (51, 52). UV—vis results showed that the absorption maxima of AuNPs-N_3 and AuNPs were both at 522 nm (Figure 2), which indicated that ligand exchange did not induce aggregation of the AuNPs.

Copper-mediated triazole cycloaddition was employed in the synthesis of AuNP aggregates at room temperature. The click reaction was visualized from the gradual color change of the solution from a wine-red suspension to dark precipitates after the addition of Cu^{2+} and NaAs into a mixture of AuNPs-N_3 and dialkynetrithiocarbonate at room temperature (Figure 3). A colorless solution was obtained after the precipitates fell down to the bottom of the vial. The appearance of the dark precipitates indicates the formation of cross-linked AuNP aggregates (Scheme 1a).

Parts c—e of Figure 1 are TEM images of AuNP aggregates prepared at different molar ratios of acetylene groups to azide groups. The molar ratio of acetylene groups to azide groups exerts a significant effect on the formation of AuNP aggregates. When the molar ratio is 1.5:1, small AuNP aggregates as well as individual AuNPs can be observed (Figure 1c). The two acetylene groups are also able to react with two azide groups on an Au-NP forming loop-like structure. In this case, only individual AuNPs with RAFT CTA on the surface are formed after click reactions. The size and density of the aggregates increase with the molar ratio. At a molar ratio of 15:1, the size of cross-linked aggregates is much bigger, and there are more AuNPs in a structure (Figure 1d). When the molar ratio reaches 30:1, the density of the structure is so high that it is hard to observe the individual AuNPs (Figure 1e). The UV—vis spectrum of the aggregates prepared at a molar ratio of 30:1 is shown in Figure 2. After click reactions, a broad plasmon band with a

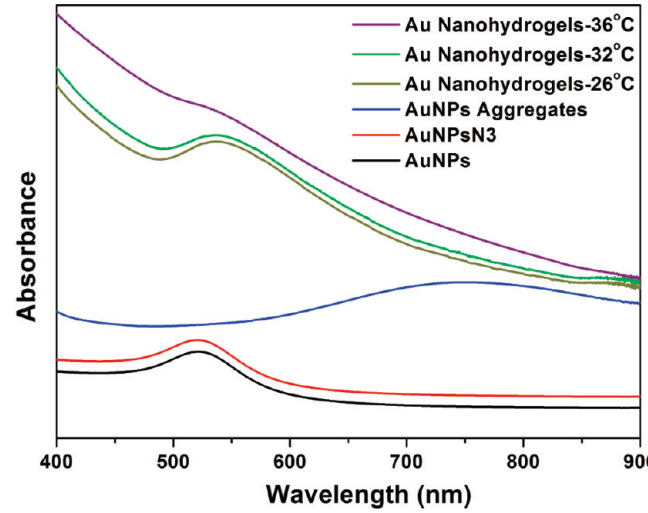

FIGURE 2. UV—vis spectra of AuNPs, AuNPs-N_3, AuNP aggregates, and AuNP nanohydrogels. In the preparation of AuNP nanohydrogels, the molar ratio of acetylene groups to azide groups was 30:1.

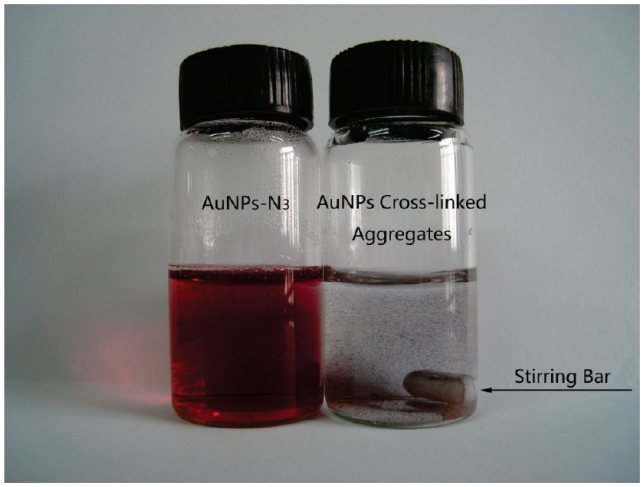

FIGURE 3. Photograph showing an aqueous dispersion of AuNPs-N_3 and dark precipitates of cross-linked AuNP aggregates.

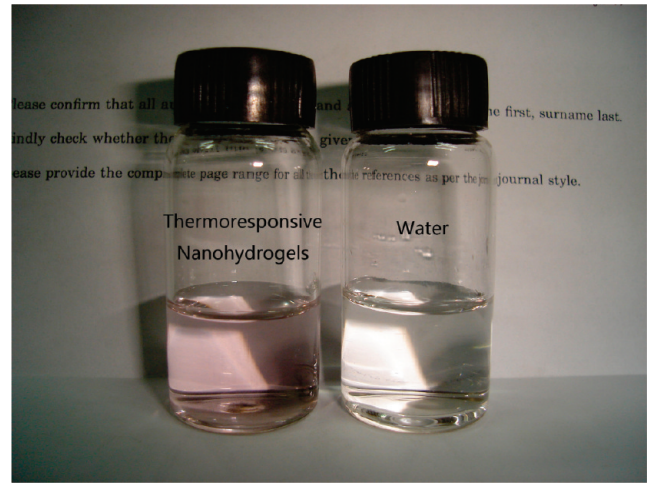

FIGURE 4. Photograph showing an aqueous solution of thermoresponsive nanohydrogels. Herein, water was used as the reference. In the nanohydrogels, the molar ratio of acetylene groups to azide groups was 30:1.

maximum at 750 nm can be observed. The red shift of the plasmon band is due to the cross-linking and high density of AuNPs in the aggregates. At a low molar ratio, only a few AuNPs were involved in an aggregate structure, so the size and cross-linking density of AuNP aggregates were low. With an increase of the amount of RAFT agent used in the click reaction, the cross-linking density and size of the aggregate structure both increased.

Thermoresponsive nanohydrogels were prepared by in situ RAFT polymerization. An NIPAM monomer and free-radical initiator ABCPA were added into an aqueous suspension of AuNP aggregates in a flask. Before polymerization, the solution was deoxygenated by bubbling through nitrogen for 1 h at room temperature. The polymerization was conducted at 100 °C for 12 h. After polymerization, the solution was dialyzed against water (MWCO = 14 000 Da) for 3 days to remove excess monomer and free-radical initiator molecules. It is worth noting that after polymerization almost all of the dark precipitates disappeared and a transparent light-purple solution was obtained at room temperature (Figure 4).

PNIPAM is a thermoresponsive polymer with a low critical solution temperature (LCST) of around 34 °C in water. The polymer undergoes phase transition at its LCST because of the cooperative dehydration of PNIPAM chains and concomitant collapse of individual chains from hydrated coils to hydrophobic globules. PNIPAM is hydrophilic below the LCST but becomes hydrophobic above that temperature (53–57). The nanohydrogels show remarkable temperature sensitivity, as manifested in their optical transmittance switching property. Figure 5 shows a plot of the temperature-dependent optical transmittance of thermoresponsive nanohydrogels. The transition temperature is determined at about 32 °C. The insets in Figure 5 are two photographs showing the solutions of thermoresponsive nanohydrogels at 20 and 45 °C. At 20 °C, a transparent solution was obtained; however, at 45 °C, the solution was cloudy. Water is a good solvent for PNIPAM at 20 °C, and polymer chains in the nanohydrogels are extended; therefore, the suspension of nanohydrogels is transparent. At 45 °C, water is a poor

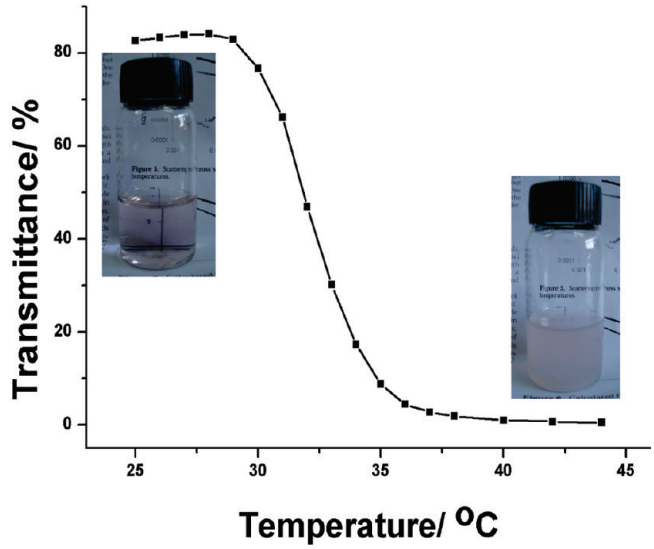

FIGURE 5. LCST curve of thermoresponsive nanohydrogels. The insets in the figure are two photographs of aqueous solutions of thermoresponsive nanohydrogels at 20 °C (transparent solution) and 45 °C (cloudy solution).

solvent for PNIPAM; PNIPAM chains collapse, undergoing "coil-to-globule" transition (58–60), so a cloudy solution was obtained. Because the AuNPs are connected by PNIPAM chains, the conformation change of PNIPAM chains will cause the size change of AuNP nanohydrogels.

The interparticle distance in the nanohydrogels has increased with growth of the PNIPAM chains. Figure 6 displays a set of representative UV–vis spectra recorded at different temperatures. At 26 °C, the absorption maximum of the AuNPs in the nanohydrogels is at 537 nm, and for AuNP aggregates, the absorption maximum is at 750 nm (Figure 2). Compared with the cross-linked AuNP aggregates, after RAFT polymerization, thermoresponsive nanohydrogels have more than 200 nm blue shift due to the extension of PNIPAM chains and the increase of the interparticle distance. Below the LCST of PNIPAM (32 °C), the maximum values of the plasmon bands of AuNPs were kept unchanged. The aqueous solution of the thermoresponsive nanohydrogels was

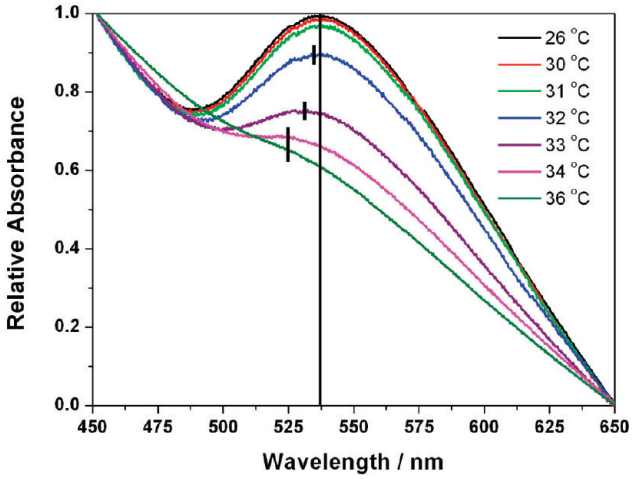

FIGURE 6. UV−vis spectra of thermoresponsive nanohydrogels recorded at different temperatures. In the preparation of AuNP nanohydrogels, the molar ratio of acetylene groups to azide groups was 30:1.

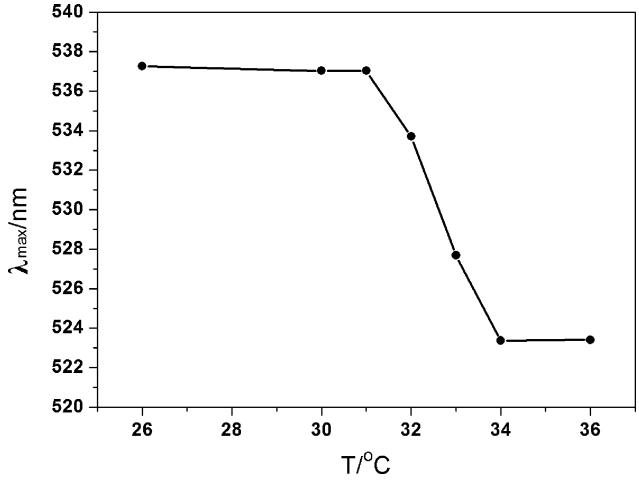

FIGURE 7. Plot indicating the shift of the absorption maxima (λ_{max}) of the plasmon bands of thermoresponsive nanohydrogels with temperature.

gradually heated above the LCST of PNIPAM. It is noted that when the temperature is above the LCST, the absorbance intensities decrease with increasing temperature. In previous research conducted by Tenhu and co-workers, similar phenomenon was also observed for AuNPs with PNIPAM brushes on the surface (61). They attributed this phenomenon to the coverage/shielding of the gold surface by collapsed PNIPAM chains. A shift of the absorption maximum of the plasmon bands of AuNPs to lower wavelengths around the LCST of PNIPAM was also observed in this research. A plot of the absorption maximum versus temperature is shown in Figure 7. The absorption maximum was kept unchanged below the LCST, and with an increase of the temperature, the absorption maximum of the plasmon bands blue-shifted to low wavelength with a transition at around the LCST of PNIPAM. The shift of the absorption maximum indicates that the surroundings of the surfaces of the AuNPs in the nanohydrogels are less hydrophilic because of the coverage of the collapsed PNIPAM chains (43, 61).

TEM was used to study the morphology of the thermoresponsive nanohydrogels. The TEM specimens were prepared by depositing an aqueous solution of nanohydrogels on Formvar grids; water was evaporated in air. Previous TEM results (Figure 1) proved that the molar ratio of acetylene groups on RAFT agents to azide groups on AuNPs played an important role in the formation of cross-linked AuNP aggregates. Because the thermoresponsive nanohydrogels were prepared from the cross-linked AuNP aggregates via RAFT polymerization, the molar ratio should also be a key factor in control of the morphology of the thermoresponsive nanohydrogels. Figure 8a presents a TEM image of thermoresponsive nanohydrogels, in which the molar ratio of acetylene groups to azide groups is 1.5:1. In the image, the PNIPAM phase and individual AuNPs in the nanohydrogels can be observed. The nanohydrogels are quite small (30−100 nm), with only a few AuNPs in a structure. With an increase of the molar ratio, the size of the thermoresponsive nanohydrogels gets bigger and bigger. When the molar ratio is 15:1, the size of the nanohydrogels ranges from 50 to 200 nm (Figure 8b). For the nanohydrogels prepared at a molar ratio of 30:1, some structures with sizes of more than 200 nm can be found (Figure 8c). With an increase of the molar ratio, there are more AuNPs in a structure. Magnified TEM images of specific nanohydrogels are presented in the insets of parts b and c of Figure 8. AuNPs in the structures can be observed.

The ζ-potential values of AuNPs and thermoresponsive nanohydrogels were also measured (Table 1). Because the AuNPs are protected by trisodium citrate on the surface, the ζ potential of the AuNPs is negative (−43 mV). After a part of trisodium citrate was exchanged by 11-azidoundecyl 2-mercaptoacetate, the ζ potential of AuNPs-N_3 was up to −40 mV. The molar ratio of acetylene groups on RAFT agents to azide groups on AuNPs exerts a significant effect on the ζ-potential values of the nanohydrogels. With an increase of the molar ratio, more RAFT agents were grafted to AuNPs, and after RAFT polymerization, there were more PNIPAM chains inside the nanohydrogels. The higher coverage of AuNPs by PNIPAM chains resulted in higher ζ-potential values.

Figure 8d is a TEM image of thermoresponsive nanohydrogels prepared at 40 °C. Compared to the nanohydrogels prepared at room temperature (Figure 8c), the size of the thermoresponsive nanohydrogels is smaller, which proves that the nanohydrogels shrink at 40 °C because of the "coil-to-globule" transition of the PNIPAM chains. Dynamic light scattering (DLS) results also indicated the thermosensitivity of the nanohydrogels. DLS curves of the thermoresponsive nanohydrogels measured at 25 and 45 °C are shown in Figure 9. When the temperature was at 25 °C (below the LCST), the hydrodynamic diameter of the nanohydrogels ranged from 180 to 279 nm, with an average value at about 228 nm; however, when the temperature was raised to 45 °C (above the LCST), the hydrodynamic diameter was in the range between 143 and 217 nm, with an average value at about 180 nm. The decrease in the size was attributed to the "coil-to-globule" transition of the PNIPAM chains.

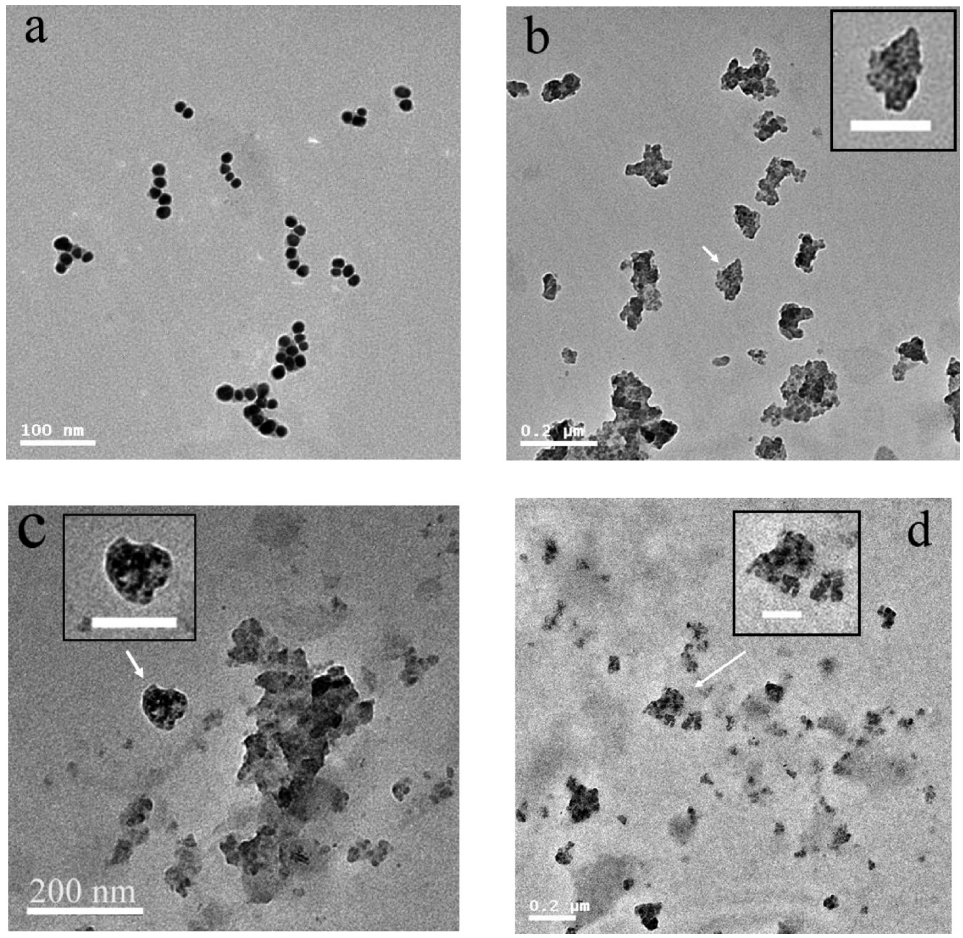

FIGURE 8. TEM images of thermoresponsive nanohydrogels with different molar ratios of acetylene to azide: (a) 1.5:1; (b) 15:1; (c) 30:1. All three specimens were prepared at room temperature. Image d is a TEM image of a specimen prepared at 40 °C. The specimen on image d has the same molar ratio of acetylene to azide as image c does. The scale bars in the insets of parts b–d represent 100 nm.

Table 1. ζ-Potential Values of AuNPs, AuNPs-N_3, and Thermoresponsive Nanohydrogels (AuNP-PNIPAM) Prepared at Different Molar Ratios of Acetylene Groups on RAFT Agents to Azide Groups on AuNPs[a]

	AuNPs	AuNPs-N_3	AuNP-PNIPAM$_1$	AuNP-PNIPAM$_2$	AuNP-PNIPAM$_3$
mean ζ potential/mV	−43.2	−40.4	−29.5	−16.8	−11.6

[a] The molar ratios of acetylene groups to azide groups in AuNP-PNIPAM$_1$, AuNP-PNIPAM$_2$, and AuNP-PNIPAM$_3$ are 1.5:1, 15:1, and 30:1, respectively.

CONCLUSIONS

To conclude, we have successfully synthesized thermoresponsive nanohydrogels based on click chemistry and RAFT polymerization. The AuNP aggregates were fabricated by a click cross-linked method between AuNPs and RAFT agents. The size of the cross-linked AuNP aggregates was determined by the molar ratio of acetylene groups on RAFT agents to azide groups on AuNPs. Three-dimensional thermoresponsive nanohydrogels were prepared by in situ RAFT polymerization of NIPAM. In water, the nanohydrogels presented a LCST at around 32 °C because of the "coil-to-globule" transition of the connecting PNIPAM chains. The size as well as the optical properties of the nanohydrogels was related to the temperature.

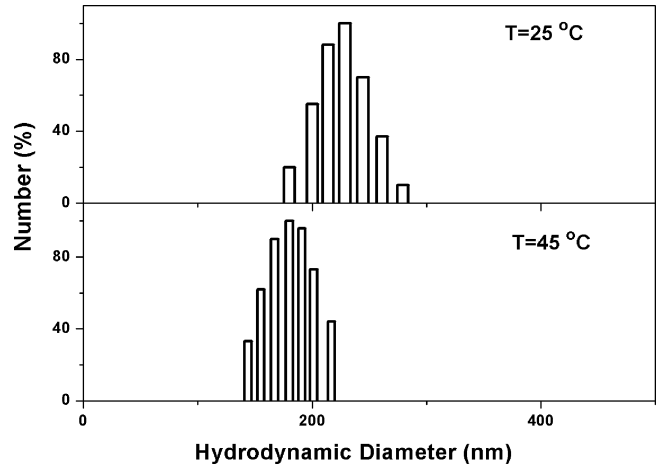

FIGURE 9. Size distributions of thermoresponsive nanohydrogels at 25 and 45 °C. In the nanohydrogels, the molar ratio of acetylene groups to azide groups was 30:1.

Acknowledgment. This project was supported by the National Natural Science Foundation of China under Contracts 20774046 and 20974047.

Supporting Information Available: ^{1}H NMR spectra of 11-azidoundecyl 2-mercaptoacetate and dialkynetrithiocarbon-

ate and more experimental data. This material is available free of charge via the Internet at http://pubs.acs.org.

REFERENCES AND NOTES

(1) Hoffman, A. S. *J. Controlled Release* **1987**, *6*, 297–305.
(2) Langer, R. *Science* **2001**, *293*, 58–59.
(3) Langer, R.; Vacanti, J. P. *Science* **1993**, *260*, 920–926.
(4) Peppas, N. A.; Hilt, J. Z.; Khademhosseini, A.; Langer, R. *Adv. Mater.* **2006**, *18*, 1345–1360.
(5) Brandl, F.; Sommer, F.; Goepferich, A. *Biomaterials* **2007**, *28*, 134–146.
(6) Graham, N. B.; Cameron, A. *Pure. Appl. Chem.* **1998**, *70*, 1271–1275.
(7) Sahiner, N.; Godbey, W. T.; McPherson, G. L.; John, V. T. *Colloid Polym. Sci.* **2006**, *284*, 1121–1129.
(8) Kuckling, D.; Vo, C. D.; Adler, H. J. P.; Voelkel, A.; Coelfen, H. *Macromolecules* **2006**, *39*, 1585–1591.
(9) Kim, S. H.; Jeong, J. H.; Chun, K. W.; Park, T. G. *Langmuir* **2005**, *21*, 8852–8857.
(10) Jung, T.; Kamm, W.; Breitenbach, A.; Kaiserling, E.; Xiao, J. X.; Kissel, T. *Eur. J. Pharm. Biopharm.* **2000**, *50*, 147–160.
(11) Oha, J. K.; Drumrighta, R.; Siegwartb, D. J.; Matyjaszewskib, K. *Prog. Polym. Sci.* **2008**, *33*, 448–477.
(12) Haraguchi, K.; Takehisa, T.; Ebato, M. *Biomacromolecules* **2006**, *7*, 3267–3275.
(13) Miyazaki, S.; Endo, H.; Karino, T.; Haraguchi, K.; Shibayama, M. *Macromolecules* **2007**, *40*, 4287–4295.
(14) Okay, O.; Oppermann, W. *Macromolecules* **2007**, *40*, 3378–3387.
(15) Haraguchi, K.; Song, L. *Macromolecules* **2007**, *40*, 5526–5536.
(16) Wang, Z.; Chen, Y. *Macromolecules* **2007**, *40*, 3402–3407.
(17) Ogoshi, T.; Takashima, Y.; Yamaguchi, H.; Harada, A. *J. Am. Chem. Soc.* **2007**, *129*, 4878–4879.
(18) Meng, L.; Lu, Y.; Wang, X.; Zhang, J.; Duan, Y.; Li, C. *Macromolecules* **2007**, *40*, 2981–2983.
(19) Oishi, M.; Tamura, A.; Nakamura, T.; Nagasaki, Y. *Adv. Funct. Mater.* **2009**, *19*, 827–834.
(20) Kawano, T.; Niidome, Y.; Mori, T.; Katayama, Y.; Niidome, T. *Bioconjugate Chem.* **2009**, *20*, 209–212.
(21) Siegwart, D. J.; Srinivasan, A.; Bencherif, S. A.; Karunanidhi, A.; Oh, J. K.; Vaidya, S.; Jin, R. C.; Hollinger, J. O.; Matyjaszewski, K. *Biomacromolecules* **2009**, *10*, 2300–2309.
(22) Oishi, M.; Hayashi, H.; Uno, T.; Ishii, T.; Iijima, M.; Nagasaki, Y. *Macromol. Chem. Phys.* **2007**, *208*, 1176–1182.
(23) Daniel, M. C.; Astruc, D. *Chem. Rev.* **2004**, *104*, 293–346.
(24) Shan, J.; Tenhu, H. *Chem. Commun.* **2007**, 4580–4598.
(25) Zhang, X.; Liu, L.; Tian, J.; Zhang, J.; Zhao, H. *Chem. Commun.* **2008**, 6549–6551.
(26) Zhang, X.; Yang, Y.; Tian, J.; Zhao, H. *Chem. Commun.* **2009**, 3807–3809.
(27) Xia, Y.; Rogers, J. A.; Paul, K. E.; Whitesides, G. M. *Chem. Rev.* **1999**, *99*, 1823–1848.
(28) Caruso, F. *Adv. Mater.* **2001**, *13*, 11–22.
(29) Shenton, W.; Davis, S. A.; Mann, S. *Adv. Mater.* **1999**, *11*, 449–452.
(30) Brown, S. *Nano Lett.* **2001**, *1*, 391–394.
(31) Frankamp, B. L.; Uzun, O.; Ilhan, F.; Boal, A. K.; Rotello, V. M. *J. Am. Chem. Soc.* **2002**, *124*, 892–893.
(32) Storhoff, J. J.; Lazarides, A. A.; Mucic, R. C.; Mirkin, C. A.; Letsinger, R. L.; Schatz, G. C. *J. Am. Chem. Soc.* **2000**, *122*, 4640–4650.
(33) Mucic, R. C.; Storhoff, J. J.; Mirkin, C. A.; Letsinger, R. L. *J. Am. Chem. Soc.* **1998**, *120*, 12674–12675.
(34) Andres, R. P.; Bielefeld, J. D.; Henderson, J. I.; Janes, D. B.; Kolagunta, V. R.; Kubiak, C. P.; Mahoney, W. J.; Osifchin, R. G. *Science* **1996**, *273*, 1690–1693.
(35) Brust, M.; Bethell, D.; Schiffrin, D. J.; Kiely, C. J. *Adv. Mater.* **1995**, *7*, 795–797.
(36) Chen, S. *Adv. Mater.* **2000**, *12*, 186–189.
(37) Liu, J.; Alvarez, J.; Ong, W.; Kaifer, A. E. *Nano Lett.* **2001**, *1*, 57–60.
(38) Kolb, H. C.; Finn, M. G.; Sharpless, K. B. *Angew. Chem., Int. Ed.* **2001**, *40*, 2004–2021.
(39) Rostovtsev, V. V.; Green, L. G.; Fokin, V. V.; Sharpless, K. B. *Angew. Chem., Int. Ed.* **2002**, *41*, 2596–2599.
(40) Fleming, D. A.; Thode, C. J.; Williams, M. E. *Chem. Mater.* **2006**, *18*, 2327–2334.
(41) Zhou, Y.; Wang, S.; Zhang, K.; Jiang, X. *Angew. Chem., Int. Ed.* **2008**, *47*, 7454–7456.
(42) Gole, A.; Murphy, C. J. *Langmuir* **2008**, *24*, 266–272.
(43) Zhang, T.; Zheng, Z.; Ding, X.; Peng, Y. *Macromol. Rapid Commun.* **2008**, *29*, 1716–1720.
(44) Pong, F. Y.; Lee, M.; Bell, J. R.; Flynn, N. T. *Langmuir* **2006**, *22*, 3851–3857.
(45) Budhlall, B. M.; Marquez, M.; Velev, O. D. *Langmuir* **2008**, *24*, 11959–11966.
(46) Karg, M.; Pastoriza-Santos, I.; Perez-Juste, J.; Hellweg, T.; Liz-Marzan, L. M. *Small* **2007**, *3*, 1222–1229.
(47) Lai, J. T.; Filla, D.; Shea, R. *Macromolecules* **2002**, *35*, 6754–6756.
(48) Frens, G. *Nature (London), Phys. Sci.* **1973**, *241*, 20–22.
(49) Quémener, D.; Davis, T. P.; Barner-Kowollik, C.; Stenzel, M. H. *Chem. Commun.* **2006**, 5051–5053.
(50) Nicolay, R.; Kwak, Y. W.; Matyjaszewski, K. *Macromolecules* **2008**, *41*, 4585–4596.
(51) Link, S.; EI-Sayed, M. A. *J. Phys. Chem. B* **1999**, *103*, 4212–4217.
(52) Link, S.; EI-Sayed, M. A. *J. Phys. Chem. B* **1999**, *103*, 8410–8426.
(53) Schild, H. G. *Prog. Polym. Sci.* **1992**, *17*, 163–249.
(54) Wu, C.; Zhou, S. *Macromolecules* **1995**, *28*, 8381–8387.
(55) Yan, J.; Ji, W.; Chen, E.; Li, Z.; Liang, D. *Macromolecules* **2008**, *41*, 4908–4913.
(56) Liang, D.; Zhou, S.; Song, L.; Zaitsev, V. S.; Chu, B. *Macromolecules* **1999**, *32*, 6326–6332.
(57) Liu, G.; Zhang, G. *J. Phys. Chem. B* **2005**, *109*, 734–747.
(58) Wang, X.; Qiu, X.; Wu, C. *Macromolecules* **1998**, *31*, 2972–2976.
(59) Wu, C.; Wang, X. *Phys. Rev. Lett.* **1998**, *80*, 4092–4094.
(60) Wang, X.; Wu, C. *Macromolecules* **1999**, *32*, 4299–4301.
(61) Raula, J.; Shan, J.; Nuopponen, M.; Niskanen, A.; Jiang, H.; Kauppinen, E. I.; Tenhu, H. *Langmuir* **2003**, *19*, 3499–3504.

AM1003156